CLM - P 28

United Kingdom Atomic Energy Authority

RESEARCH GROUP

Preprint

EXPERIMENTAL STUDY OF FAST HYDROMAGNETIC WAVES IN AN ARGON PLASMA

D. F. JEPHCOTT
A. MALEIN

Culham Laboratory,

Culham, Abingdon, Berkshire

1963

UNCLASSIFED
(Approved for Publication)

CLM - P 28

EXPERIMENTAL STUDY OF FAST HYDROMAGNETIC WAVES IN AN ARGON PLASMA*

by

D.F. JEPHCOTT
A. MALEIN

*A preliminary report of this work was given at the 4th Annual Meeting of the Division of Plasma Physics of the American Physical Society in Atlantic City, November, 1962.

U.K.A.E.A. Research Group,
Culham Laboratory,
Nr. Abingdon,
Berks.

August, 1963

(C/18) I.M.G.

ABSTRACT

In these experiments fast hydromagnetic waves are excited by discharging a capacitor through a single turn coil surrounding a cylindrical column of magnetised argon plasma. The plasma column is 200 cm long and 22 cm in diameter, and the axial magnetic field strength is varied in the range from 1 to 6 kG. The wave amplitude is typically 10 G, and the frequency is varied between 1.2 and 6 times the ion cyclotron frequency. Measurement of the radial variation and the relative amplitudes of the three components of the wave magnetic field shows that the oscillation is the lowest axially-symmetric mode. As predicted by the theory, the wave is elliptically polarised in the $r\theta$ plane with the magnetic vector rotating in the same sense as the electron cyclotron rotation. The experimental results demonstrate the cut-off of this mode both as the frequency is decreased and as the axial magnetic field strength is increased. Measurements of the axial wave number and absorption coefficient are in good numerical agreement with theoretical dispersion curves computed from the measured plasma parameters.

This work provides quantitative evidence to support the theories currently used in treating hydromagnetic oscillations, both stable and unstable, of magnetised plasmas.

C O N T E N T S

1. INTRODUCTION

The experimental study of waves in plasmas provides important guidance on the approximations which can be used in treating theoretically the response of a magnetised plasma to small perturbations. A correct choice of these approximations is necessary for the understanding of the instabilities which have so far prevented the magnetic confinement of plasmas for generating controlled thermonuclear reactions.

The theory of hydromagnetic wave propagation in a cylindrical plasma has been investigated by Baños (1955), Newcomb (1957), Stix (1957)(1958), Lehnert (1959), Gajewski (1959) and by many others. A precise treatment of the problem, in which all the dissipative and resonance effects are included, has been carried out by Woods (1962). The theoretical dispersion curve has two branches, corresponding to two distinct modes of oscillation which we call the slow and fast waves. The slow wave propagates only at angular frequencies ω below the ion cyclotron frequency ω_{ci}, and is a simple torsional oscillation when $\omega \ll \omega_{ci}$. The fast wave propagates only if $\omega > k_c v_A$, where k_c is the radial wave number and v_A is the Alfvén speed. For $\omega \ll \omega_{ci}$ it is a simple compressional wave with phase velocity $v_{ph} = \omega(\omega^2/v_A^2 - k_c^2)^{-\frac{1}{2}}$. If $\omega \gg \omega_{ci}$ and the axial wave number $\eta \gg k_c$, then the phase velocity is $v_{ph} = (\omega/\omega_{ci})^{\frac{1}{2}} v_A$, the ions take no part in the wave motion, and the wave then corresponds to the whistler mode predicted by the Appleton-Hartree dispersion relation. Dissipative effects in the plasma give rise to wave damping, which reduces the sharpness of the resonance regions where wave propagation ceases.

Experiments concerned with the slow wave have been reported by Allen et al. (1959), Jephcott (1959), Nagao & Sato (1960), Hooke et al.

(1961), Sinelnikov et al. (1961), Wilcox et al. (1961) and Jephcott & Stocker (1962). The whistler mode ($\omega \gg \omega_{ci}$) has been studied by Storey (1953) and by Dellis & Weaver (1962). Some observations on the fast hydromagnetic wave ($\omega \approx \omega_{ci}$) have been carried out by Kovan et al. (1961) and Hooke et al. (1962), but so far no extensive study of this wave has been reported. In this paper we present the results of a detailed investigation of the fas wave in an argon plasma. The object of this work is twofold; first to provide experimental confirmation of the main properties predicted for the wave, and second to provide a detailed numerical check on the theory. Extensive measurements of the plasma properties have been made, and it is established that no gross non-uniformities exist within the plasma. Thus a comparison between the measurements on the wave and Woods's precise theory can be made without the use of fitted parameters and with some confidence that the experimental medium matches the theoretical model of a uniform plasma completely filling the discharge tube.

2. APPARATUS

A scale diagram of the experiment is shown in figure 1. The discharge tube consists of a 22 cm bore glass cylinder, 200 cm long, fitted with stainless steel disc electrodes at each end and with a coaxial return conductor. This assembly is mounted in a solenoid connected to a 200 kJ capacitor bank which provides an axial magnetic field up to 6 kG with a rise time of 2 ms. The magnetic field is uniform to within 2% throughout the volume of the discharge tube. Argon gas flows continuously through the tube at a pressure of 50 mTorr, and the gas discharge current is supplied by a 12 kJ capacitor bank switched across the electrodes. The gas current rises to a maximum of 20 kA in 140 μs, coinciding with the maximum of the

axial magnetic field. Both capacitor banks are short-circuited at the time of maximum current; the magnetic field and gas current then decay exponentially. Oscillograms of the axial magnetic field and the discharge current are shown in figure 2, which also indicates the time chosen for the wave excitation, 400 μs after the start of the decay. By this time the gas current has decreased to about 5 kA and the plasma is relatively quiescent. Experimental measurements are recorded over a 10 μs interval; during this time the gas current decreases by 3% and the axial magnetic field by 0.1%. Changes in the experimental conditions during the 10 μs interval are negligible.

A 120 cm long cylinder of brass mesh is fitted closely round the outer wall of the discharge tube. The time taken for magnetic flux to penetrate the cylinder is about 100 μs, thus for the experimental range of wave frequencies (200 kc/s to 1 Mc/s) the brass cylinder acts as an electrically conducting boundary, but it produces negligible distortion in the slowly rising axial magnetic field.

3. WAVE EXCITATION

The hydromagnetic wave is excited in a region 50 cm from one end of the discharge tube where the plasma is free from non-uniformities and impurities associated with the electrodes. A 10 J capacitor in series with an inductor network is discharged through a single wire loop round the tube circumference; this circuit is allowed to oscillate freely. The current in the loop excites an $m = 0$ fast wave which propagates along the tube with a frequency equal to that of the exciter system. The inductor network is adjusted to give wave frequencies between 200 kc/s and 1 Mc/s, and the peak current in the exciter loop is about 1 kA. The exciter circuit has a Q value of about 30 at all frequencies used, so the bandwidth of frequencies present in the decaying oscillation is about 3% of the central

frequency.

4. WAVE DETECTION

The oscillating magnetic field of the wave is detected by search coils, 5 mm in diameter, placed at different axial positions along the tube. All measurements of wave parameters are taken with the search coils at least 20 cm inside the ends of the brass cylinder which forms the conducting boundary section of the tube. The coils are protected from the plasma by quartz sheaths, and can be moved across the tube diameter to measure the radial structure of the wave. In a typical experiment the wave amplitude varies up to a maximum of about 1·0 G; this is less than 1% of the axial magnetic field strength. The mean power dissipated by the wave in the plasma is at the most 0.05 watt cm^{-3} for a period of 100 μs; this is not sufficient to raise the electron temperature by more than 0.05 eV and it is shown later that it does not produce any significant change in the plasma density.

Figure 3(a) shows an oscillogram of the signals from two search coils of equal sensitivity, spaced 12 cm apart on the tube axis, detecting the z component of a 256 kc/s wave in plasma with an ion number density $n_i = 1.3 \times 10^{15}$ cm^{-3} and an axial magnetic field of 4 kG. The wave amplitude builds up during the first few cycles and then follows the pattern of the decaying exciter current. The regularity of the signals, which are not integrated, indicates the absence of gross instabilities in the discharge. A spark gap in the exciter circuit produces high frequency interference at the start of the traces; this has been removed by a low-pass filter which attenuates frequencies higher than 4 Mc/s. Figure 3(b) shows the signals obtained when the axial magnetic field is increased to 6 kG, all other conditions remaining unchanged. The 256 kc/s exciter frequency

is now below the cut-off frequency and the signals show a transient oscillation containing frequencies higher than 256 kc/s merging into a low amplitude 256 kc/s signal. The transient signal arises from the high frequency components present in the initial sharp rise of the exciter current and the low amplitude 256 kc/s wave appears because the cut-off is not perfect in a dissipative medium. Experimental measurements are taken from the signals arriving after the wave builds up to maximum amplitude.

The time taken for any particular wave peak to travel the distance between the two coils gives the phase velocity v_{ph}, and the axial wave number is $\eta = \omega/v_{ph}$. Four measurements of the time delay between corresponding peaks in the upper and lower signals are made on each of 10 oscillograms taken from successive discharges; the 40 measurements are averaged to obtain one experimental point. The measured values of η are independent of the distance between the search coils and of their axial position within the conducting boundary section of the tube.

The decrease in amplitude as the wave travels along the tube gives the absorption coefficient ε; values of ε are calculated from the relative amplitudes of the wave peaks used to measure η. With low wave frequencies the absorption coefficients obtained in this way are independent of the distance between the coils, but at high frequencies the absorption coefficient apparently changes with the coil separation; this may be caused by standing waves between electrostatic screens which surround the coils. To avoid errors arising from this effect the absorption coefficient at high wave frequencies is obtained from 40 measurements of the wave amplitude at each of five different axial positions, using a single search coil. When two coils are used, errors caused by any difference in the sensitivity of the coils and

oscilloscope amplifiers are eliminated by interchanging the coils and amplifiers half way through each set of measurements.

Errors arising from the assumption that the wave is monochromatic, i.e. from ignoring the 3% bandwidth, are negligible because the medium is not highly dispersive. The maximum error in any single reading from an oscillogram is generally less than 5%, thus averaging over 40 measurements virtually eliminates reading errors. The standard errors given in the results arise almost entirely from variations between waves observed in different discharges.

5. PLASMA PROPERTIES

To compare the experimental results with theory we must know the numerical values of the plasma parameters which appear in the dispersion equation, i.e. the electrical conductivities $\sigma_{\parallel}$ and $\sigma_{\perp}$ parallel and perpendicular to the axial magnetic field, the ion and neutral atom number densities n_i and n_n, and the frequency ω_{in} with which positive ions collide with neutral gas atoms. We must also investigate the experimental plasma to find how closely it matches the theoretical model of a uniform plasma completely filling the tube.

Measurements of the plasma properties at the time of wave propagation are described briefly below; these measurements are independent of axial magnetic field changes in the range from 1.5 kG to 6 kG.

(a) The radial variation in the azimuthal magnetic field of the discharge current is measured by moving a search coil across the tube diameter. This measurement shows that the discharge current density is uniform to within ± 5% across the tube diameter, except close to the walls where the current density falls to zero across a boundary layer which is less than 1 cm thick. The same radial variation in current density is found at three different axial positions along

the tube.

(b) The electrical conductivity of the plasma is found from electrostatic probe measurements of the axial electric field and search coil measurements of the discharge current density. The conductivity, averaged over the tube cross-section including the boundary layer, is $\sigma_{\parallel} = 57 \pm 4\ \Omega^{-1}\ cm^{-1}$, and we assume $\sigma_{\perp} = \sigma_{\parallel}/2$ (Spitzer 1956). The corresponding electron temperature is $T_e = 1.5 \pm 0.1$ eV. The error quoted is the maximum error, which arises mainly from the large radial gradient in discharge current density near the tube wall.

(c) A time-resolved spectrum of the radiation from a cylinder of plasma about 1 cm in diameter, extending along the axis of the discharge tube, is obtained by optically sweeping the spectrum down a photographic plate. The plate is exposed for 100 discharges and the spectrum covers the wavelength range from 2,200 Å to 6,500 Å. At the time of wave propagation the radiation is almost entirely from singly ionised argon atoms. No emission is detected from neutral argon or from multiply ionised argon. Calculations show that the ratio of multiply ionised to singly ionised argon atoms is less than 10^{-3} (Berg 1963), and absence of neutral atoms in the main body of the plasma is consistent with earlier experimental observations on the slow hydromagnetic wave in a similar discharge, where neutral argon atoms were apparently lost to the tube wall during the discharge (Jephcott & Stocker 1962).

(d) The mean number density n_e of electrons on the tube axis is determined by a new method in which a He-Ne gas laser is used as an infra-red interferometer (Ashby & Jephcott 1963). Because there is no multiple ionisation, the ion number density n_i is equal to the electron number density. This measurement gives n_i on the tube axis equal to $1.5 \pm 0.05 \times 10^{15}\ cm^{-3}$ (standard error of 20 measurements).

A sensitive means of detecting any significant change in plasma density caused by energy dissipation from the wave would be to observe a difference in electron density between discharges with and without the wave propagating. The laser measurement, capable of detecting changes in n_e as small as 5%, shows no difference between the two cases. We therefore assume that the wave does not significantly alter the electron and ion number densities.

(e) A floating Langmuir double probe (Johnson & Malter 1950) is used to check the uniformity of the electron temperature and ion number density. Probe characteristics are plotted for 7 different radial positions and for 3 points along the tube axis. The usual difficulty in interpreting Langmuir probe characteristics to obtain absolute measurements of n_i does not arise because the probe is calibrated by the laser measurement. For tube radii from 0 to 10 cm these measurements give $n_i = 1.4 \pm 0.1 \times 10^{15}$ cm^{-3} and $T_e = 1.2 \pm 0.1$ eV, which agrees with the electron temperature calculated from $\sigma_{//}$ to within 25%. At a few mm from the tube wall we measure $n_i = 1.0 \pm 0.1 \times 10^{15}$ cm^{-3} and $T_e = 0.9 \pm 0.1$ eV. The value of n_i averaged over the tube cross-section is $1.3 \pm 0.1 \times 10^{15}$ cm^{-3}. The errors here arise from radial gradients in n_i and T_e; no axial gradients in these parameters are detected.

(f) The number density of neutral atoms in the plasma is not known but we can calculate an approximate maximum value of the ion-neutral collision frequency. We assume that no neutral argon atoms are dislodged from the tube wall during the discharge; the spectroscopic evidence provides support for this assumption. The collision frequency is given approximately by $\omega_{in} = n_n \sigma_m v_i$, where σ_m is the momentum transfer cross-section and v_i is the mean thermal velocity of the ions. Since the initial atom number density corresponding to

a pressure of 50 mTorr is 1.8×10^{15} cm^{-3}, we have $n_n \approx 5 \times 10^{14}$ cm^{-3}. We take $\sigma_m = 1.3 \times 10^{-14}$ cm^2 (Hornbeck 1951), and if we assume the ion temperature $T_i \leq T_e$ then $v_i \leq 3 \times 10^5$ cm sec^{-1}. From these figures we obtain $\omega_{in} \leq 2 \times 10^6$ sec^{-1}. We shall show later that, with this value of ω_{in}, collisions between ions and neutral atoms do not play an important part in the experiment.

At this point it is useful to summarise the information we have on the uniformity of the 80 cm length of plasma column in which the wave measurements are made. The axial magnetic field is uniform in space to within 2% and decreases by 0.1% in the 10 μs interval used for the wave measurements; during this time the discharge current falls by 3%. Changes in the ion number density, electron temperature and electrical conductivity, with time and with axial position along the tube are negligible compared with the radial gradients in these quantities. The discharge current density, the ion number density and electron temperature, are uniform to within 8% for radii from 0 to 10 cm but drop sharply between 10 cm radius and the wall at 11 cm. Thus the plasma can be regarded as an essentially uniform cylinder about 20 cm in diameter surrounded by a somewhat cooler boundary layer, about 1 cm thick, in contact with the tube wall.

For the plasma parameters given above, the pressure and viscosity terms in the dispersion relation (equation (27) of Woods 1962) are negligible. The plasma pressure is about three orders of magnitude less than the magnetic field pressure and, assuming that $T_i = T_e$ and that the axial magnetic field does not reduce the plasma viscosity, the maximum viscous damping of the wave is calculated to be about three orders of magnitude less than the resistive damping. The dispersion relation therefore reduces to Woods's equation (60):-

$$\{sk^2 - k_A^2(1 + \frac{ik^2}{\sigma_\perp \omega} + \frac{ik_c^2}{\sigma_{\parallel} \omega})\}\{s(k^2 + k_c^2) - k_A^2(1 + \frac{ik^2}{\sigma_\perp \omega} + \frac{ik_c^2}{\sigma_\perp \omega})\} = k^2(k^2 + k_c^2)(\frac{\omega}{\omega_{ci}})^2$$

where s ≡ the ion neutral collision term, a complex quantity. (For a fully ionised gas, $s = 1$.)

$k \equiv \eta + i\varepsilon$

η ≡ the axial wave number.

ε ≡ the absorption coefficient.

$k_A \equiv \frac{\omega}{v_A}$

k_c ≡ the radial wave number.

6. WAVE MODE

For the lowest $m = 0$ mode, the radial variation in amplitude of the $r\ \theta$ and z components of the wave magnetic field is given by Woods's equation (82):-

$$B_{1r} = - i \eta A J_1(k_c r)$$

$$B_{1\theta} = \frac{\eta(\eta^2 + k_c^2)}{k_A^2 - s_1 \eta^2} \cdot \frac{\omega}{\omega_{ci}} A J_1(k_{cr})$$

$$B_{1z} = k_c A J_o(k_c r)$$

where s_1 is the real part of s, and A is the common amplitude factor.

The determination of the radial wave number k_c from the boundary conditions is discussed in detail by Woods. For a tube with conducting walls the boundary conditions are such that B_{1r} $B_{1\theta}$ and the radial current density j_{1r} are all zero at the tube wall. In the experiment we have a boundary consisting of the conducting cylinder separated from the plasma by the 3 to 4 mm wall thickness of the glass discharge tube. At the glass wall j_{1r}, and therefore $B_{1\theta}$, must be zero while B_{1r} and B_{1z} can penetrate as far as the conductor. Thus we might expect a radial variation in wave amplitude

similar to that for a tube with conducting walls but with some distortion in the wave pattern close to the wall.

The radial variation in the three components of the wave magnetic field has been measured under the following experimental conditions:-

Axial magnetic field $B_o = 4.0$ kG

Wave frequency $\omega = 1.6 \times 10^6$ rad sec^{-1}

Ion cyclotron frequency $\omega_{ci} = 0.97 \times 10^6$ rad sec^{-1}

Axial wave number $\eta = 0.15$ cm^{-1}
(measured experimentally)

Radial wave number $k_c = 0.35$ cm^{-1}
(assuming a conducting boundary at r = 11 cm)

Ion number density $n_i = 1.3 \times 10^{15}$ cm^{-3}
(from laser and Langmuir probe measurements.)

Substituting these values in Woods's equation (82) we have:-

$B_{1r} : B_{1\theta} : B_{1z} = -i0.43\, J_1(0.35r) : 0.68\, J_1(0.35r) : J_o(0.35r)$.

Thus, according to the theory, the wave should be elliptically polarised in the $r\theta$ plane with the magnetic vector rotating in the same sense as the electron cyclotron motion. Measurement of the relative phases and amplitudes of B_{1r} and $B_{1\theta}$ confirms that this elliptical polarisation does exist experimentally and that the magnetic vector rotates in the expected sense. The elliptical polarisation is illustrated by the oscillograms in figures 4(a) and 4(b) showing signals from two equally sensitive search coils which detect B_{1r} and $B_{1\theta}$ at the same point in the plasma, half way along the conducting wall section of the tube and at a radius of 5.3 cm. Figure 4(a) shows the normal situation in which the smaller amplitude B_{1r} signal (lower trace) is $\pi/2$ in advance of the larger amplitude $B_{1\theta}$ signal (upper trace). If the probe is left in the same position but the direction of the axial magnetic field is reversed, then the phase relationship reverses as shown in figure 4(b).

The curves in figure 5 represent the theoretical amplitudes, $0.43\ J_1\ (0.35r)$, $0.68\ J_1\ (0.35r)$ and $J_o\ (0.35r)$, of B_{1r} $B_{1\theta}$ and B_{1z}; these curves are normalised by putting the amplitude factor A equal to unity. The experimental points each represent the average of 10 successive measurements and the standard error varies up to $\pm$ 10%. The measured amplitude of B_{1z} on the tube axis is normalised to unity, and the other measured amplitudes are multiplied by the same normalising factor. The experimental measurements show that the radial pattern of the wave and the amplitude ratio of the three components correspond closely to the theoretical predictions for the lowest $m = 0$ mode bounded by a conducting wall.

When the conducting cylinder is removed, the radial variation in wave amplitude undergoes a marked change. The B_{1r} and B_{1z} components penetrate well beyond the insulating glass wall while $B_{1\theta}$ remains zero at the wall, thus the wave no longer consists of a single mode of oscillation. This observation is in accord with Woods's theory, which shows that the boundary conditions for a tube with insulating walls cannot be satisfied by a single mode of oscillation, except under conditions such that $B_{1\theta}$ is negligibly small at all radii.

To avoid the complication of dealing with multiple modes of oscillation we have confined our other experimental measurements to the case with the conducting cylinder in position. In comparing these measurements with theory we neglect the non-uniformity of the plasma boundary layer and assume that the glass wall is replaced by a conductor at $r = 11$ cm. The complex boundary must give rise to effects not considered in the theory, but does not appear to cause any marked distortion in the wave pattern.

In the above discussion of the wave mode, and in the following

sections, we assume for simplicity that k_c is a real number throughout the experimental range; this assumption is valid providing the ratio $\eta/\varepsilon \gg 1$. In the experiment, we have $\eta/\varepsilon \approx 10$ in regions well removed from the cut-off, but the ratio decreases and becomes nearly unity at cut-off.

7. DISPERSION CURVES

The dispersion of the hydromagnetic wave is examined in two ways:-

(a) by measuring the axial wave number η at different wave frequencies ω, with the axial magnetic field B_o kept constant, and

(b) by measuring η at different values of B_o, with constant ω.

These measurements are compared with solutions of Woods's dispersion equation computed from the experimentally observed values of the plasma parameters.

The curves in figure 6 represent solutions for η as a function of ω, using 5 different values of the ion number density n_i, with the experimental parameters $B_o = 4.0$ kG, $\sigma_{\parallel} = 57\ \Omega^{-1}\ cm^{-1}$ and $k_c = 0.35\ cm^{-1}$. The independent variable ω is plotted as the ordinate to give a conventional dispersion curve. The effect of including the finite plasma conductivity is to reduce the sharpness of the cut-off at $\omega = k_c v_A$, and η reaches a small value but does not become zero. The lower set of experimental points are the observed values of η in the plasma with a measured value of $n_i = 1.3 \times 10^{15}\ cm^{-3}$. Each point represents the average of 40 measurements, and the standard error is indicated by limit bars. The discrepancy between theory and experiment is less than 10%. The upper set of measurements shows the effect of reducing the initial pressure in the discharge tube from 50 mTorr to 25 mTorr. With the reduced pressure the ion number density on the axis, measured by the laser, is $0.94 \pm 0.05 \times 10^{15}\ cm^{-3}$. Because of the probable

decrease in ion density close to the wall we expect the mean ion density to be somewhat less than this; the experimental points lie close to the curve calculated for $n_i = 0.8 \times 10^{15}$ cm^{-3}.

In calculating the theoretical curves in figure 6 it is assumed that there are no neutral gas atoms present in the plasma. If the ion-neutral collision term is included in the dispersion equation, using the calculated maximum value of the ion-neutral collision frequency $\omega_{in} = 2 \times 10^6$ sec^{-1}, then the theoretical values of η increase by between 5% and 20% as ω decreases below 2×10^6 rad sec^{-1}. The change in η is negligible for $\omega > 2 \times 10^6$ rad sec^{-1}; this is because the ions take a decreasing part in the wave motion as $\frac{\omega}{\omega_{ci}}$ increases above unity, and the effect of collisions between ions and neutral gas atoms therefore decreases as the frequency is raised.

Figure 6 shows the cut-off as ω is decreased towards $\omega_o = k_c v_A$. Figure 7 shows the approach to cut-off when ω is kept constant at 1.6×10^6 rad sec^{-1} and v_A is increased by raising the axial magnetic field strength B_o. The curve represents the dispersion equation solutions for η as a function of B_o, using the measured parameters $n_i = 1.3 \times 10^{15}$ cm^{-3}, $\sigma_{\parallel} = 57\ \Omega^{-1}$ cm^{-1} and $k_c = 0.35$ cm^{-1}. Again we have good numerical agreement between the theoretical curve and the measured values of η. The lowest measured value of η occurs at $B_o = 5.5$ kG; at higher magnetic fields the wave amplitude is too low for measurements to be made.

8. WAVE DAMPING

The wave damping is investigated under the same experimental conditions as those used for the measurements of η. The curve in figure 8 represents the dispersion equation solutions for the

absorption coefficient ε as a function of ω, with the experimental parameters $B_o = 4.0$ kG, $n_i = 1.3 \times 10^{15}$ cm^{-3}, $\sigma_{\parallel} = 57\ \Omega^{-1}$ cm^{-1} and $k_c = 0.35$ cm^{-1}. A sharp increase in ε occurs as ω decreases towards the cut-off frequency $\omega_o = k_c v_A$. The ion-neutral collision term is again not included in calculating this theoretical curve. Calculations in which the maximum value of the ion-neutral collision frequency is included show that the maximum effect would be to increase the calculated values of ε by about 10% for $\omega > 1.8 \times 10^6$ rad sec^{-1}; at lower frequencies the effect is negligible. Thus the damping is almost entirely due to resistive dissipation in the plasma, and the presence of any neutral gas atoms can be ignored. The experimental points in figure 8 each represent the average of at least 40 successive measurements. The discrepancy between theory and experiment is 25% at the worst point, and is about 10% over most of the experimental range. The fact that the four upper experimental points all lie on the same side of the theoretical curve may however indicate a systematic error.

In figure 9, the curve shows the calculated values of ε as a function of B_o using in the dispersion equation the observed parameters $\omega = 1.6 \times 10^6$ rad sec^{-1}, $n_i = 1.3 \times 10^{15}$ cm^{-3}, $\sigma_{\parallel} = 57\ \Omega^{-1}$ cm^{-1} and $k_c = 0.35$ cm^{-1}. The cut-off is indicated by the increase in ε as the magnetic field increases in the region of $B_o = 5$ kG. The experimental measurements are in good numerical agreement with the theoretical curve, the discrepancy generally being less than 10%.

9. CONCLUSIONS

This work confirms the main features theoretically predicted for the fast hydromagnetic wave. In spite of the complex physical nature of the boundary in the experiment, measurements of the radial variation in the three components of the wave magnetic field, and their relative

amplitudes, correspond closely to the theoretical pattern for the lowest $m = 0$ mode in a tube with electrically conducting walls. The wave is elliptically polarised in the $r\theta$ plane, and the magnetic vector rotates in the same sense as the electron cyclotron rotation. The cut-off theoretically predicted for the fast wave is observed experimentally. Measurements of the axial wave number and the absorption coefficient agree with solutions of the dispersion equation computed from the measured plasma parameters. Those discrepancies which do occur are in general less than 10%, and may be attributed to experimental errors rather than to any fault in the theory.

The most important feature of this work is the support which it provides for the theories currently used in treating hydromagnetic oscillations, both stable and unstable, of magnetised plasmas.

We thank Mr. A.I. Kilvington and Mr. C.F. Parker for their valuable contribution to the experiment. We are also grateful for many useful discussions with Dr. R.J. Bickerton and Dr. L.C. Woods.

REFERENCES

Allen, T.K., Baker, W.R., Pyle, R.V. and Wilcox, J.M. 1959 Phys. Rev. Lett. 2, 383.

Ashby, D.E.T.F. & Jephcott, D.F. 1963 Appl. Phys. Lett. 3, 13.

Baños, A. 1956 Proc. Roy. Soc. A233, 350.

Berg, H. 1963 private communication.

Dellis, A.N. & Weaver, J.M. 1962 Nature, 193, 1274.

Gajewski, R. 1959 Phys.Fluids, 2, 633.

Hooke, W.M., Tenney, F.H., Brennan, M.H., Hill, H.M. and Stix, T.H. 1961 Phys. Fluids, 4, 1131.

Hooke, W.M., Rothman, M.A., Avivi, P. & Adam, J. 1962 Phys. Fluids, 5, 864.

Hornbeck, J.A. 1951 Phys. Rev. 84, 615.

Jephcott, D.F. 1959 Nature, 183, 1652.

Jephcott, D.F. & Stocker, P.M. 1962 J. Fluid Mech. 13, 587.

Johnson, E.O. & Malter, L. 1950 Phys. Rev. 80, 58.

Kovan, I.A., Patrushev, B.I., Rusanov, V.D., Smirnov, V.P. & Frank-Kamenetsky, D.A. 1961 Paper 205, I.A.E.A. Conf. Plasma Physics and Controlled Nuclear Fusion Research, Salzburg.

Lehnert, B. 1959 Supplement to Vol.XIII, Serie X, Del Nuovo Cimento, 59.

Nagao, S. & Sato, T. 1960 J. Phys. Soc. Japan 15, 735.

Newcomb, W.A. 1957 Magnetohydrodynamics, p.109. Stanford University Press.

Sinelnikov, K.D., Tolok, V.T., Nazarov, N.I., Ermakov, A.I., Lodko, A.C. & Bondrev, V.A. 1961 Paper 231, I.A.E.A. Conf. Plasma Physics and Controlled Nuclear Fusion Research, Salzburg.

Spitzer, L. 1956 Physics of Fully Ionised Gases. New York : Interscience.

Stix, T.H. 1957 Phys. Rev. 106, 1146.

Stix, T.H. 1958 Phys. Fluids, 1, 308.

Storey, L.R.O. 1953 Phil. Trans. Roy. Soc. A246, 113.

Wilcox, J.M., De Silva, A.W. & Cooper, W.S. 1961 Phys. Fluids, 4, 1506.

Woods, L.C. 1962 J. Fluid Mech. 13, 570.

FIGURE LEGENDS

1. Scale diagram of apparatus

2. Upper trace, axial magnetic field; base line at centre of graticule.

   Centre trace, discharge current

   Lower trace, exciter current

   Sweep speed, 100 μs per large division.

3(a) Magnetic probe signals, $\omega = 1.6 \times 10^6$ rad sec^{-1}, $\omega > k_c v_A$. Sweep speed, 5μs per large division.

3(b) Magnetic probe signals, $\omega = 1.6 \times 10^6$ rad sec^{-1}, $\omega < k_c v_A$. Sweep speed, 5μs per large division.

4(a) Upper trace, $B_{1\theta}$. Lower trace, B_{1r}. Axial magnetic field normal.

4(b) Upper trace, $B_{1\theta}$. Lower trace, B_{1r}. Axial magnetic field reversed.

5. Radial variation in B_{1r} $B_{1\theta}$ and B_{1z}.

6. η as $f(\omega)$; $B_o = 4$ kG.

7. η as $f(B_o)$; $\omega = 1.6 \times 10^6$ rad sec^{-1}.

8. ε as $f(\omega)$; $B_o = 4$ kG,

9. ε as $f(B_o)$; $\omega = 1.6 \times 10^6$ rad sec^{-1}.

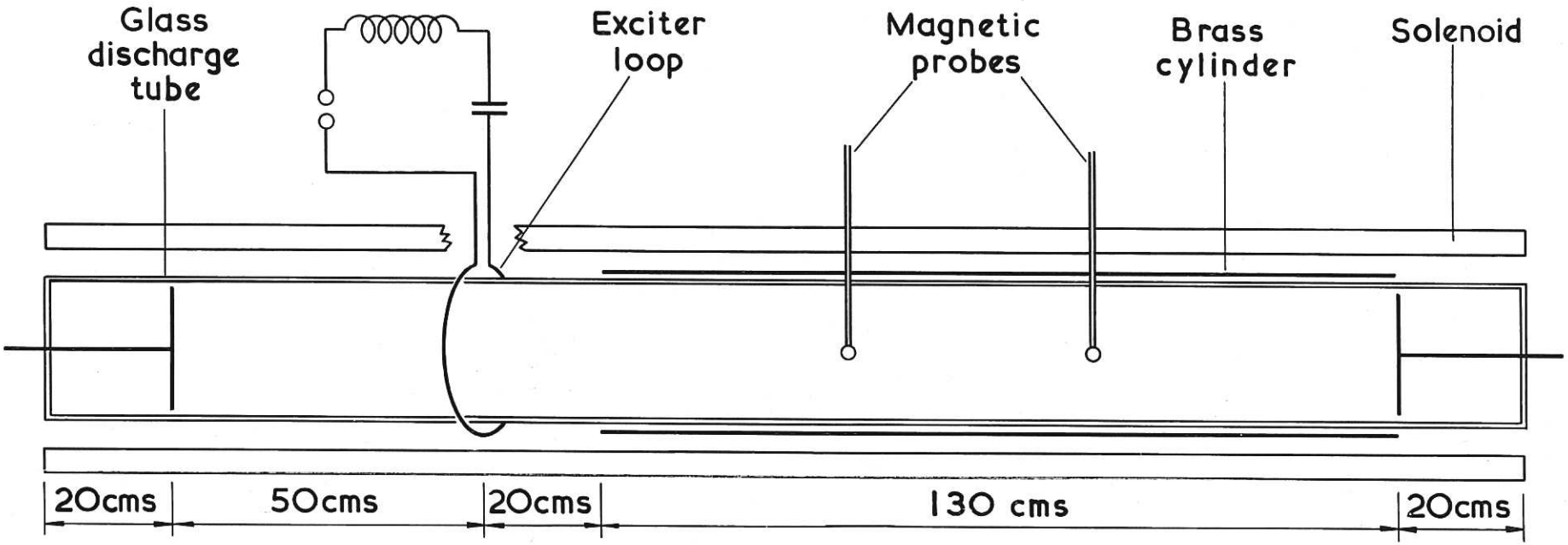

CLM- P 28 Fig. 1 Scale diagram of apparatus.

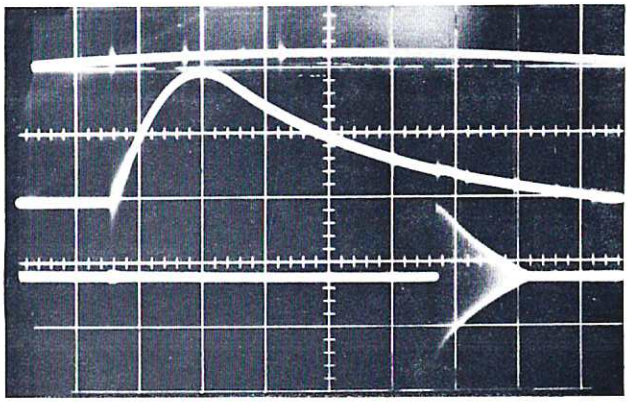

CLM - P 28 Fig. 2 Upper trace, axial magnetic field; base line at centre of graticule.

Centre trace, discharge current

Lower trace, exciter current.

Sweep speed, 100μs per large division.

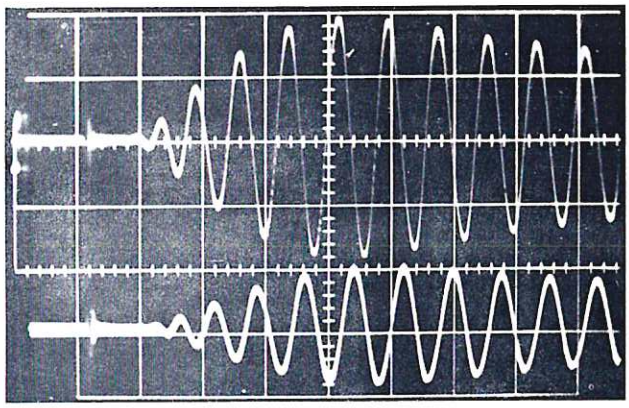

CLM - P 28 Fig. 3a Magnetic probe signals, $\omega = 1.6 \times 10^6$ rad sec^{-1}, $\omega > k_c v_A$.
Sweep speed, 5μs per large division.

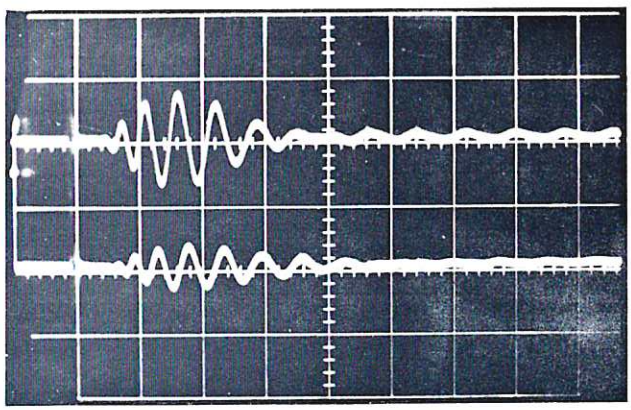

CLM - P 28 Fig. 3b Magnetic probe signals, $\omega = 1.6 \times 10^6$ rad sec^{-1}, $\omega < k_c v_A$.
Sweep speed, 5μs per large division.

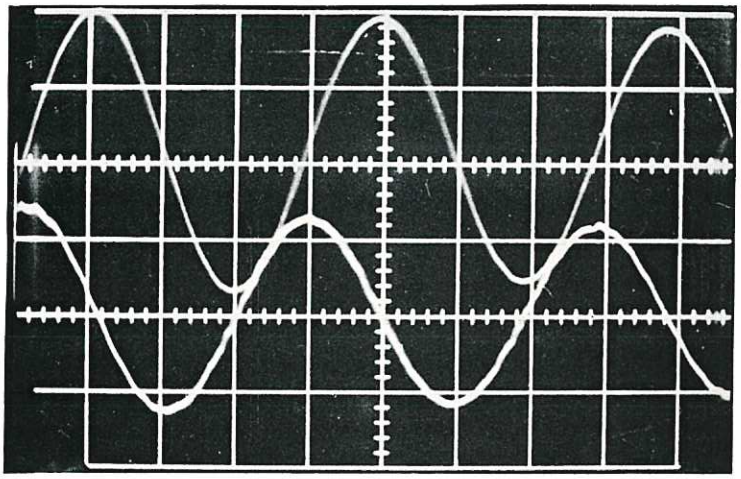

CLM- P 28 Fig. 4a

Upper trace, $B_{1\theta}$. Lower trace, B_{1r}. Axial magnetic field normal.

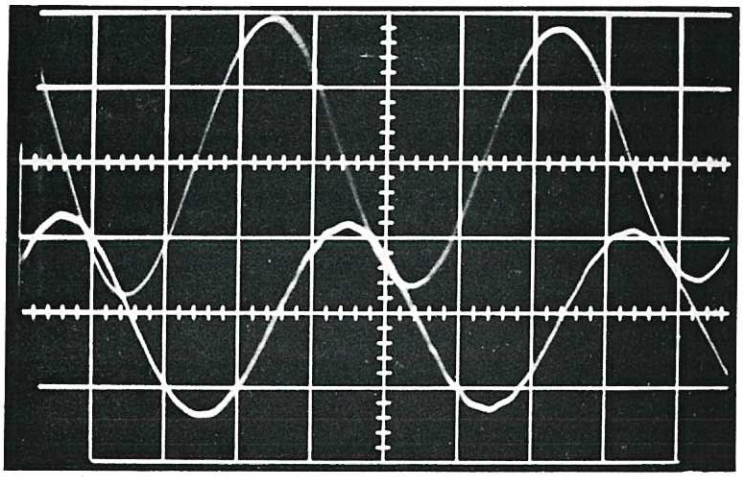

CLM- P 28 Fig. 4b

Upper trace, $B_{1\theta}$. Lower trace, B_{1r}. Axial magnetic field reversed.

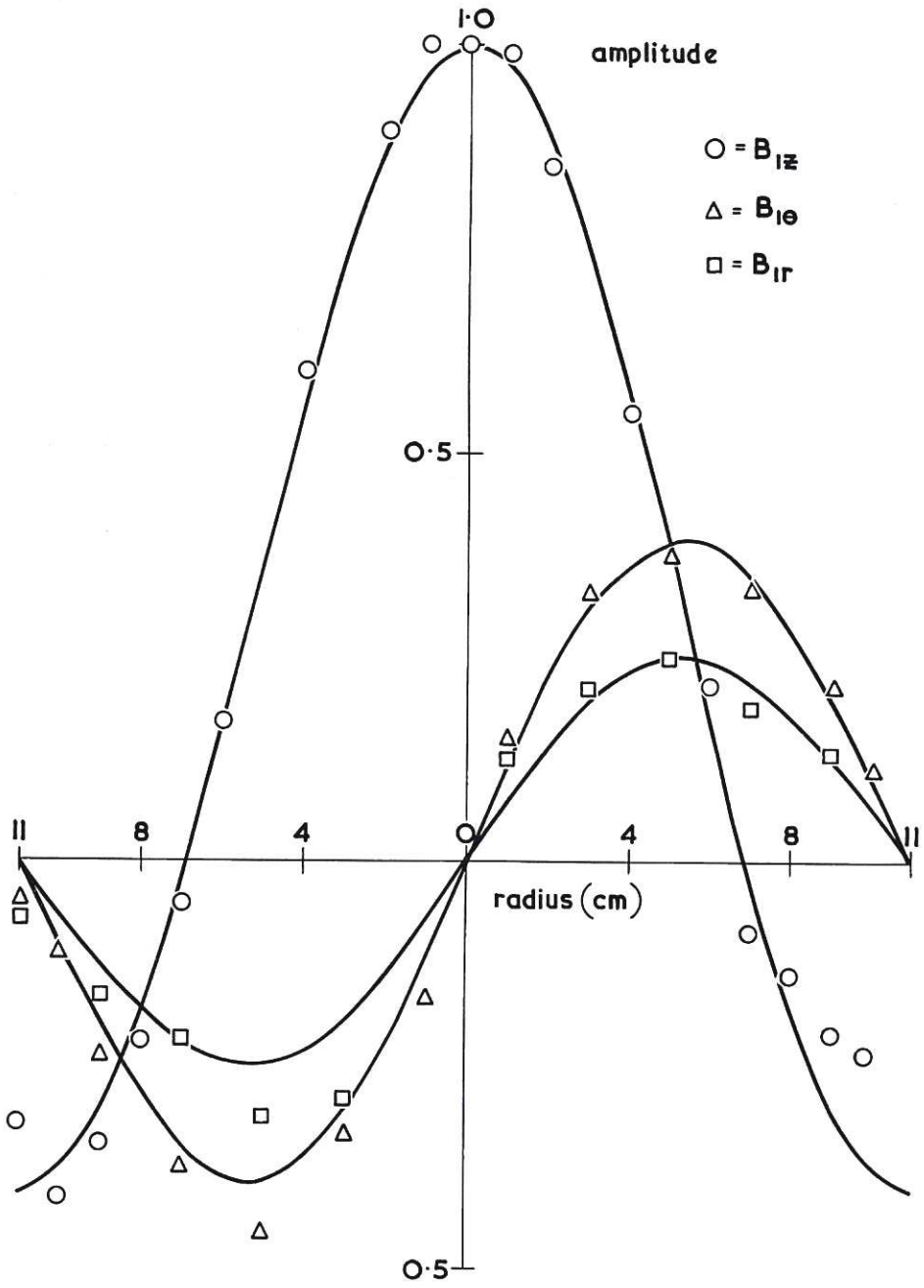

CLM- P 28 Fig. 5 Radial variation in B_{1r} $B_{1\theta}$ and B_{1z}.

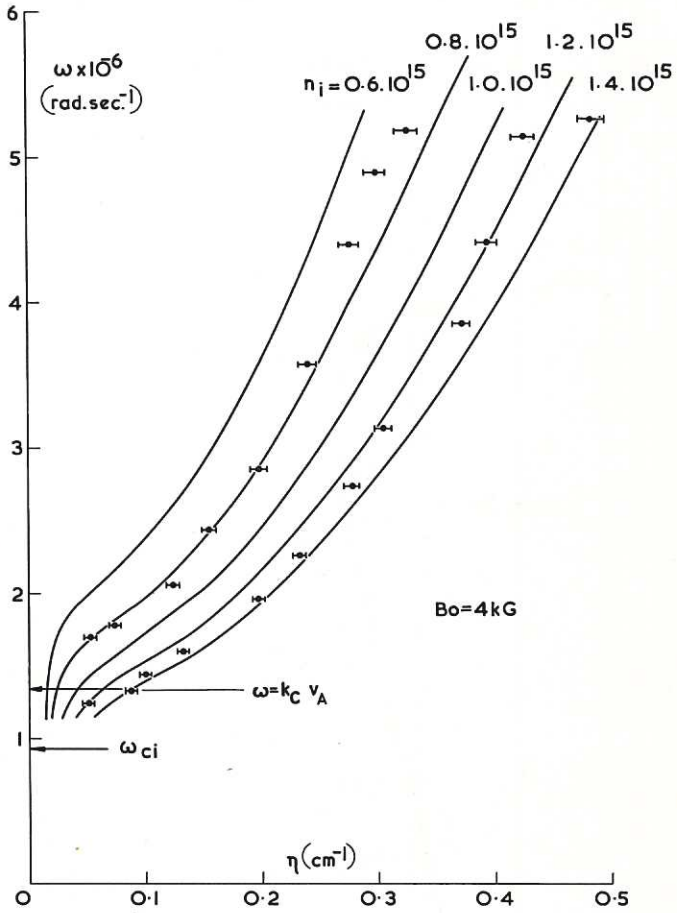

CLM- P28 Fig. 6 η as f(ω) ; B_0 = 4 kG.

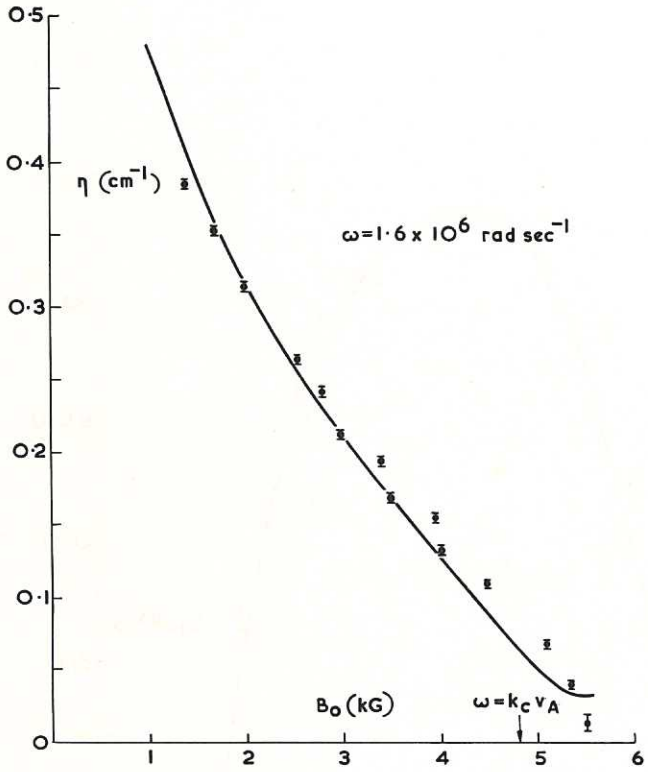

CLM- P28 Fig. 7 η as f(B_0) ; $\omega = 1.6 \times 10^6$ rad sec^{-1}.

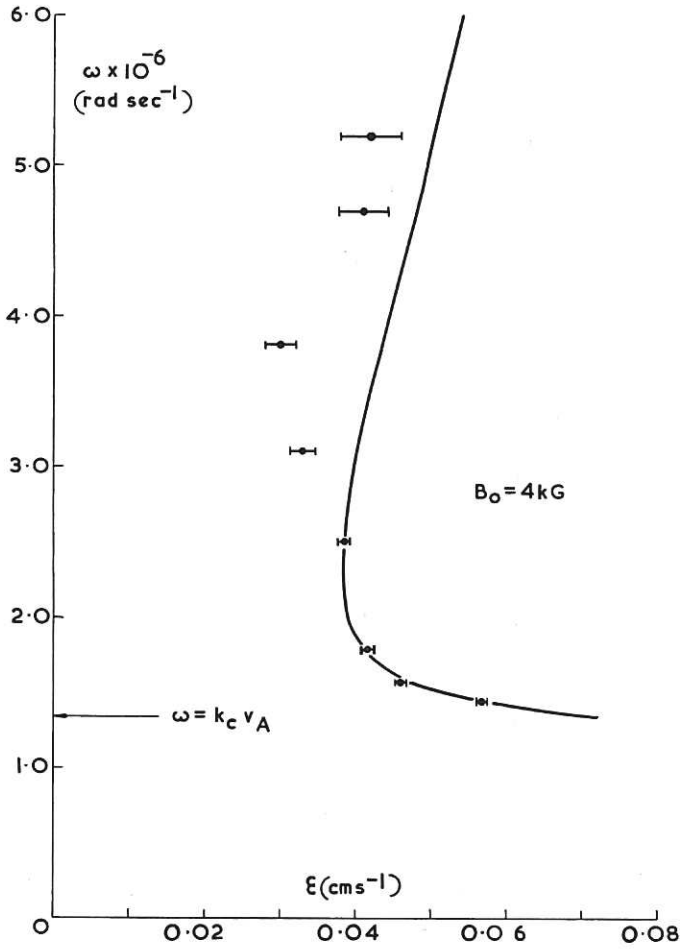

CLM- P28 Fig. 8 ϵ as f(ω) ; B_0 = 4 kG.

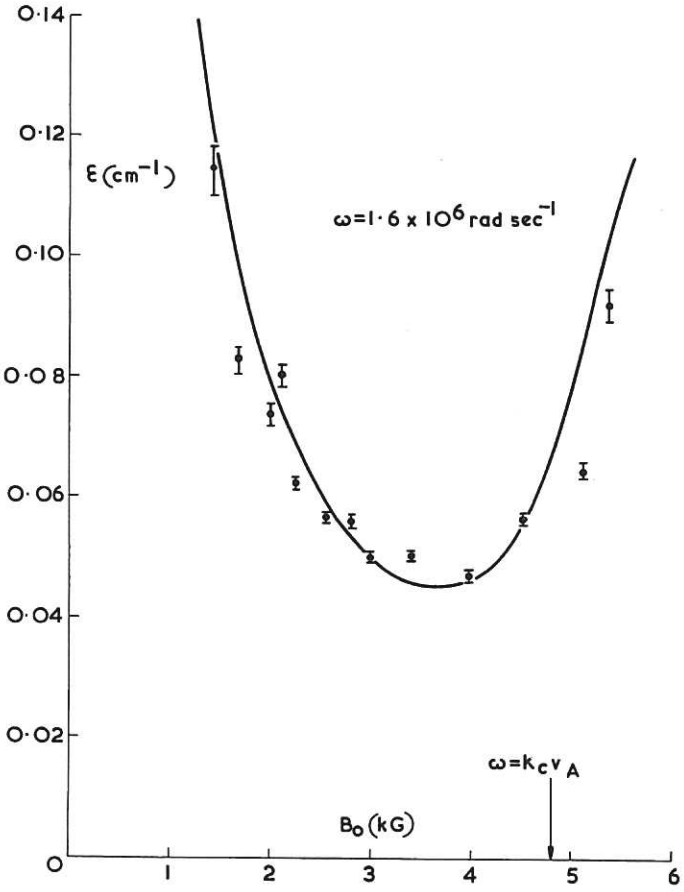

CLM- P28 Fig. 9 ϵ as f(B_0) ; $\omega = 1.6 \times 10^6$ rad sec^{-1}.